Tellus (1990), *42A*, 508–519

Distributions of available potential and kinetic energy budget quantities associated with wintertime cyclone activity along the eastern coasts of Asia and North America

By JOHN V. ZAPOTOCNY, *Department of Atmospheric Sciences, Creighton University, California at 24th Street, Omaha, Nebraska 68178, USA*

(Manuscript received 10 June 1988; in final form 14 February 1990)

ABSTRACT

Available potential energy and kinetic energy budget quantities are examined during a two-week period of the Global Weather Experiment (GWE) winter season (14–28 February 1979) for regions encompassing the cyclogenetically active eastern coasts of Asia and North America. Twice daily values of vertically integrated available potential energy generation, kinetic energy generation, and kinetic energy boundary flux are produced using gridded isentropic data derived from the National Meteorological Center's Level IIIa set of global analyses. Available potential energy generation is found on average to be positive in the North American study region but negative in the East Asian domain, indicating net destruction of baroclinicity by the diabatic heating distribution in that sector of the northern hemisphere during the period. Spatial distributions of time-averaged available potential energy generation show little relationship to cyclone tracks in the North American or Asian study regions. However, the patterns of time-averaged kinetic energy generation correspond quite well to areas of rapid cyclone deepening and cyclone decay. In addition, temporal changes in regionally integrated kinetic energy generation values indicate that a strong rise in kinetic energy production accompanied each major cyclogenesis event within the study regions. Time series of the kinetic energy boundary flux reveal that the North American region is a net exporter of kinetic energy during the two-week study period. The Asian region is found to import more kinetic energy than it exports, thus representing a sink of kinetic energy for the northern hemisphere as a whole during the latter half of February 1979.

1. Introduction

Climatological studies of winter season extratropical cyclone activity have shown that the eastern coasts of Asia and North America are among the most cyclogenetically active portions of the northern hemisphere (Klein, 1957; Zishka and Smith, 1980; Whittaker and Horn, 1982, 1984). Fig. 1 shows the principal areas of cyclone formation in these regions during the wintertime. Among the features contributing to the predominance of cyclogenesis along these coastlines are enhanced coastal baroclinic zones maintained by the strong thermal contrast between the cold continents to the west and the relatively warm oceans to the east. As first shown by Margules (1903), it is the vast supply of total potential (internal plus gravitational potential) energy stored within the baroclinic configuration of the atmosphere that provides the ultimate source of kinetic energy for extratropical storms. Lorenz (1955a), in expanding upon the work of Margules, defined the atmospheric property available potential energy which helps to quantify the amount of baroclinic energy within an atmospheric domain that may be utilized for kinetic energy production during cyclogenesis.

Numerous studies have examined the planetary and hemispheric distributions of available potential energy and kinetic energy (Oort, 1964; Peixoto and Oort, 1974; Oort and Peixoto, 1976; Min and Horn, 1982) as well as the energetics of

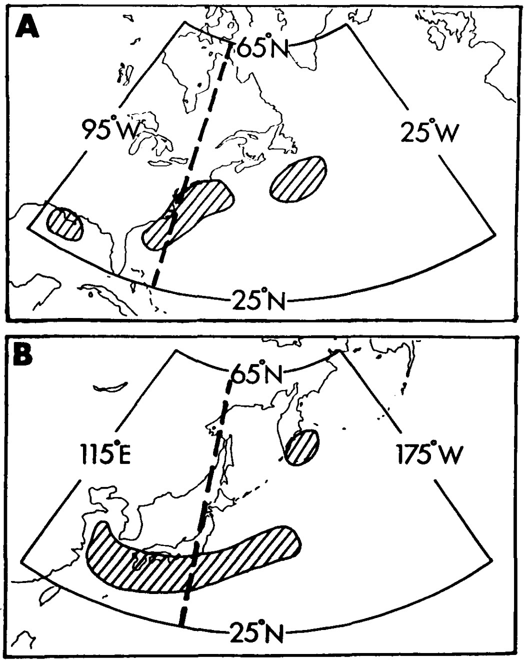

Fig. 1. Sectors of the northern hemisphere used in this study, the eastern coast of North America (a) and of Asia (b). Dashed lines at 75° W in (a) and at 140°E in (b) locate the meridional cross sections shown in Fig. 2. Hatched areas indicate the principal regions of cyclogenesis during the month of February (from Whittaker and Horn, 1982).

individual storm systems (Hahn and Horn, 1969; Johnson, 1970; Bullock and Johnson, 1971a and 1971b; Gall and Johnson, 1971). Still other research has focused on the budgets of available potential energy and kinetic energy within atmospheric domains on the scale of individual cyclone systems as well as for the global atmosphere (Min and Horn, 1974; Chen et al., 1978; Alpert, 1981; Kung and Chan, 1981; Lin and Smith, 1982; Cressman, 1984). To date, however, relatively little attention has been given to the problem of relating distributions of available potential energy and kinetic energy budget parameters to patterns of extratropical cyclone development and movement on a regional scale over a time period spanning several storm life-cycles. In an effort to better understand the role energy generations and transports play in maintaining regional-scale environments conducive to cyclogenesis, the present study examines spatial and temporal patterns of available potential energy and kinetic energy budget quantities associated with cyclone activity along the eastern coasts of Asia and North America (Fig. 1) during a cyclogenetically active two-week period (14–28 February 1979) of the Global Weather Exeriment (GWE) year (December 1978–November 1979). Specifically, this paper focuses on the spatial distributions of available potential energy generation and the spatial and temporal patterns of kinetic energy generation as related to cyclones within the two study regions. The interaction between these cyclogenetically active east coast regions and their larger-scale environments is also examined through the exchange of kinetic energy across the domain boundaries. The energy budget quantities are calculated according to the isentropic formulations developed by Johnson (1970) using data derived from the Level IIIa analyses prepared by the United States National Meteorological Center (NMC). This research represents an extension of a previously published paper (Zapotocny, 1987) which examines the spatial distributions of vertically integrated available potential energy and kinetic energy accompanying cyclones in the two east coast study regions.

2. Budget equations

Johnson (1970) obtained expressions whereby the energetics of an open system can be explicitly separated from the global domain. The equations for the time rate of change of regional available potential energy can be written

$$\mathrm{d}A/\mathrm{d}t = G(A) + S(A), \tag{1}$$

where $G(A)$ represents the generation of available potential energy within the volume, and $S(A)$ symbolizes all other sources of regional available potential energy. $S(A)$ can be expressed as

$$S(A) = B(A) + W(A + K) - S(K). \tag{2}$$

Here, $B(A)$ is the advection of available potential energy into the volume, $W(A + K)$ is the pressure work done by the environment on the boundaries of the domain and $S(K)$ is the generation of kinetic energy within the volume by the ageostrophic component of motion. In a similar fashion, the budget equation for kinetic energy can be written

$$\mathrm{d}K/\mathrm{d}t = S(K) + B(K) + D(K), \qquad (3)$$

where $B(K)$ is the advection of kinetic energy into the volume and $D(K)$ is the viscous dissipation of kinetic energy within the volume.

It is important to point out that the local production of kinetic energy [$S(K)$] within an open system need not be realized only from the direct conversion of available potential energy to kinetic energy within the volume; but rather, as noted by Johnson (1970) and Johnson and Downey (1982), may be associated both with boundary processes, $B(A)$ and $W(A+K)$, and the conversion of in situ available potential energy. Only if the sum of $B(A)$ and $W(A+K)$ vanishes will a given increase in kinetic energy cause a decrease of equal magnitude in the available potential energy of the system.

A complete diagnosis of the energy budget for any open system requires inclusion of all terms listed in eqs. 1, 2 and 3 above. However, in this study only the $G(A)$, $S(K)$ and $B(K)$ terms have been quantified and examined. Consider first the isentropic expression for generation of kinetic energy. It can be written as

$$S(K) = -\frac{1}{g}\int_{A_\theta}\int_{\theta_s}^{\theta_t} \boldsymbol{V}\cdot\nabla\Psi\,\frac{\partial p}{\partial\theta}\,\mathrm{d}\theta\,\mathrm{d}A_\theta \qquad (4)$$

where $\boldsymbol{V}$ is the vector wind and $\nabla\Psi$ is the gradient of Montgomery streamfunction on an isentropic surface, g is the acceleration of gravity, θ is potential temperature, θ_s and θ_t represent the potential temperature at the surface of the earth and top of the domain respectively, and A_θ is the surface area of the region over which the integration is being done. The boundary advection of kinetic energy is

$$B(K) = \frac{1}{g}\oint_L\int_{\theta_s}^{\theta_t} k\,\frac{\partial p}{\partial\theta}\,\boldsymbol{V}\cdot\boldsymbol{n}\,\mathrm{d}\theta\,\mathrm{d}L. \qquad (5)$$

Here the symbol $\oint$ represents a closed integration around the lateral boundary of the volume L, $\boldsymbol{n}$ is a unit vector which is everywhere normal to the vertical walls of the volume pointing outward and k is specific kinetic energy. A net zero flux is assumed at the bottom of a domain. The vertical advection through the top boundary is also neglected since computations show it to be at least two orders of magnitude smaller than the horizontal advection. Finally, the generation term for available potential energy is expressed in isentropic coordinates as

$$G(A) = -\frac{1}{g}\int_{A_\theta}\int_{\theta_s}^{\theta_t}\{1-(p_r/p)^\kappa\}\,Q_m\,\frac{\partial p}{\partial\theta}\,\mathrm{d}\theta\,\mathrm{d}A_\theta \qquad (6)$$

where Q_m is the per unit mass rate of diabatic heating. The term in brackets, known as the efficiency factor,

$$\varepsilon = \{1-(p_r/p)^\kappa\} \qquad (7)$$

is a measure of the effectiveness of diabatic heating in generating available potential energy within the volume. Here p is pressure, p_r is the reference pressure on an isentropic surface, and κ is the ratio of the dry air gas constant R_d to the specific heat of air at constant pressure c_p. For a given distribution of heating or cooling, $G(A)$ is a function of the distribution of pressure on isentropic surfaces. Positive generation results if heating occurs where the pressure exceeds the reference value ($p > p_r$, $\varepsilon > 1$) or when cooling is applied where the pressure is less than the reference pressure ($p < p_r$, $\varepsilon < 1$). The generation of available potential energy within a volume is therefore dependent on the three dimensional covariance of heating and efficiency factor.

3. Data and computational methods

In practice, the equations described above for computing $G(A)$, $S(K)$ and $B(K)$ (eqs. (4)–(6)) must be evaluated in finite difference form, meaning that an areal and vertical summation must be performed for each of the 493 (29×17) individual gridbox domains comprising the study regions. Gridded isentropic data for the calculations were generated through a vertical interpolation of the NMC Level IIIa set of isobaric analyses from the GWE year (Townsend and Johnson, 1985). The interpolation algorithm is based upon the assumption that potential temperature (θ) varies linearly in the vertical with p^κ ($\kappa = R_d/c_p$). This is a reasonable assumption if sufficient vertical resolution in potential temperature is used when performing the interpolation. A total of 16 isentropic levels were produced with 10 K vertical resolution. The original 2.5° latitude–longitude horizontal resolution was maintained. Isentropic data at each level consist of

u and v component winds, pressure, relative humidity and Montgomery streamfunction. Surface values of these parameters are also available along with values of the surface potential temperature. To insure that the full depth of the troposphere was included in the study domains the top isentropic level was specified as 370 K, corresponding to a pressure level of approximately 150 mb. This is well above the middle latitude wintertime tropopause level. For a further description of the basic NMC Level IIIa data see Bergman (1979) and McPherson et al. (1979).

The reference pressure used for computing the efficiency factor is easily calculated in the free atmosphere as the area-averaged pressure on an isentropic surface. An iterative method devised by Koehler (1986) was used to calculate reference pressures for those isentropic levels which intersect the ground. Distributions of mass-weighted diabatic heating (Q_m) required for the determination of available potential energy generation were obtained through a technique similar to that used by Wei et al. (1983). In this method, the isentropic equation of mass continuity is evaluated to obtain distributions of 12-hourly diabatic mass flux through isentropic surfaces at 10 K intervals. From these, vertical profiles of per unit mass diabatic heating can be determined for each $2.5° \times 2.5°$ gridbox and used together with the three-dimensional distributions of efficiency factor to calculate 12-h average $G(A)$ values for the gridbox.

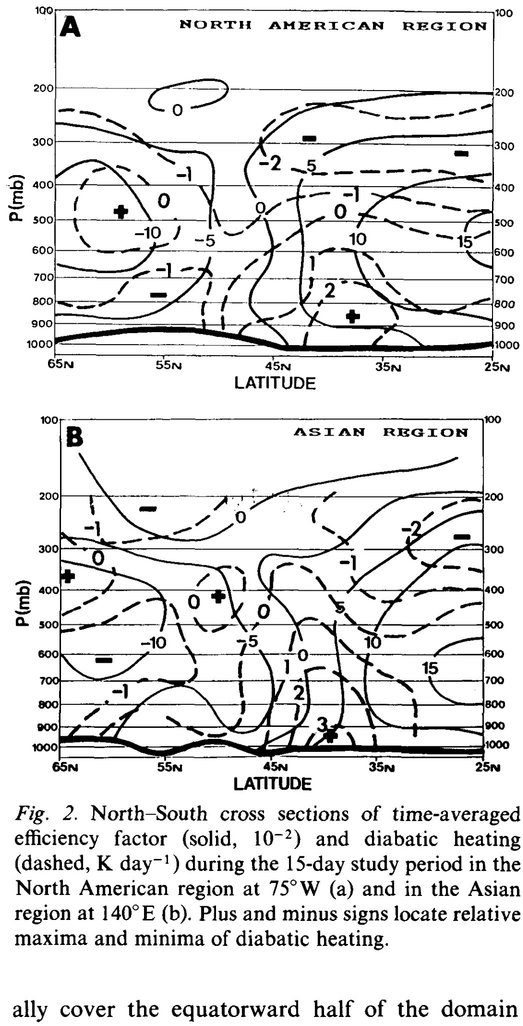

Fig. 2. North–South cross sections of time-averaged efficiency factor (solid, 10^{-2}) and diabatic heating (dashed, K day^{-1}) during the 15-day study period in the North American region at 75°W (a) and in the Asian region at 140°E (b). Plus and minus signs locate relative maxima and minima of diabatic heating.

4. Distributions of time-averaged energy generations

Recall that the generation of available potential energy within an atmospheric volume is dependent upon the three dimensional covariance of diabatic heating and efficiency factor. Because ε is a function of reference pressure, $G(A)$ also depends on the changing distribution of p_r within the volume. Fig. 2 shows cross sections of time-averaged efficiency factor and diabatic heating rates for each region. The cross sections are N–S oriented along the continental coastlines at longitudes of 75°W and 140°E in the North American and Asian regions, respectively. In both cross sections, positive values of $\bar{\varepsilon}$ generally cover the equatorward half of the domain with negative values over the poleward half. A weak secondary area of positive mean efficiency factor is located above the tropopause in the northern portion of both cross sections. The horizontal gradient of $\bar{\varepsilon}$ in the lower troposphere is somewhat stronger in the Asian region than in the North American region, indicating the stronger N–S baroclinic zone along the Asian coast. The magnitudes of $\bar{\varepsilon}$ are largest in the middle troposphere; thus, heating or cooling at these levels would be more effective in generating available potential energy than at other levels. For a further discussion of the role of efficiency factor distributions in the generation of available potential energy see Lorenz (1955b), Bullock and Johnson (1971a, 1971b), Gall and Johnson

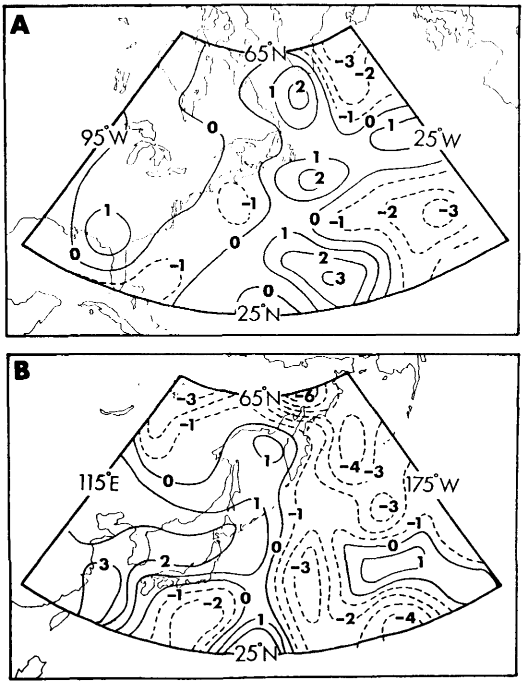

Fig. 3. Distributions of time-averaged, vertically integrated generation of available potential energy [$G(A)$] in the North American region (a) and Asian region (b) (10 W m^{-2}).

(1971), Min and Horn (1974) or Lin and Smith (1982).

In general, the distributions of diabatic heating (Fig. 2) show positive values in the southern portion of the regions and negative values (cooling) over about the northern half of the regions. Local diabatic tendencies were computed, as described earlier, using the isentropic equation of mass continuity as applied by Wei et al. (1983). No attempt has been made in this study to reduce the total diabatic tendency into its sensible and latent heating components. The distributions and magnitudes of diabatic heating obtained in the present evaluation compare favorably with those obtained from previous studies of heating distributions in these regions (Min and Horn, 1974; Schaack and Johnson, 1986; Johnson, 1989) and appear reasonable.

The 12-h mean values of $G(A)$ were vertically integrated and time-averaged for the entire 15-day period to arrive at the distributions of time mean available potential energy generation shown in Fig. 3. The patterns of time mean $G(A)$ are poorly organized with multiple maxima and minima in each region. The only coherent areas of positive mean generation extend along the Asian coast from China northeastward to the Kamchatka Peninsula, and in a N–S band over the central North Atlantic Ocean extending southward from Greenland. Comparison of these analyses with the cyclone tracks during the study period (Fig. 4) does not indicate any clear correspondence between the distributions of available energy generation and cyclone activity. In fact, the only indication of a systematic relationship is the tendency for positive mean $G(A)$ values poleward of the corridors of most frequent activity in the Asian region with negative values on the equatorward side. Little, if any, relationship is noted in the North American region. It is important to remember that energy generations associated with cyclones represent a transient phenomenon which will not necessarily be apparent in time-averaged results. Recently, Ponater and Speth (1984) examined the conversions from available potential energy to kinetic energy within the northern hemisphere. They found that the transient component of energy conversion was more than double the local time-averaged, or standing, component with maximum transient contributions along the eastern coasts of Asia and North America. It is not unreasonable to expect a similar situation with regard to energy generation patterns.

Monthly mean generations of available potential energy during the wintertime along the eastern coasts of Asia and North America have been previously studied by Min and Horn (1974). Their computations were based upon sounding data for December and January averaged for a period of several years. Results showed areas of strong positive mean available energy generation along the North American coast near Cape Hatteras and along the Asian coast near Japan. The area of positive mean $G(A)$ along the Asian coast noted in the present study (Fig. 3) agrees with these earlier findings. However, a region of negative mean $G(A)$ exists along the North American coast where Min and Horn found strong positive generation. This difference is possibly related to the comparative lack of strong cyclogenesis along the immediate North American east coast during the February study

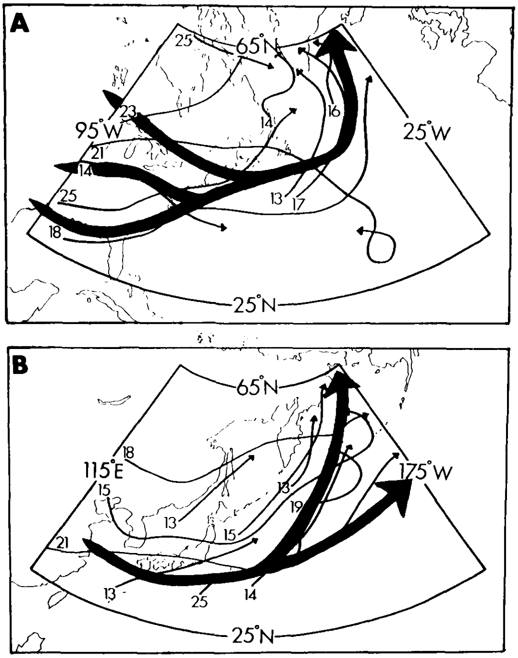

Fig. 4. Cyclone tracks during the 15-day study period in the North American region (a) and Asian region (b). Numbers indicate the date of cyclone formation of movement into the region. Bold lines depict mean cyclone tracks for February (from Whittaker and Horn, 1982).

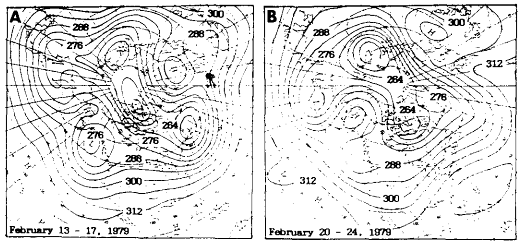

Fig. 5. Northern hemisphere 5-day mean 700 mb geopotential heights (dm) for 13–17 February 1979 (a) and 20–24 February 1979 (b) (from Dickson, 1979).

period (Koehler and Min, 1984). As indicated in Fig. 4, no cyclones formed along the immediate east coast of the United States during the study period. Most of the storms originated either in the lee of the Rocky Mountains or out to sea south of the Canadian maritime provinces and Greenland. This is not to say that cyclogenesis was entirely absent along the North American coast. Indeed, rapid intensification of at least two cyclones occurred in this area; however, the origination of coastal storms was certainly less prevalent than along the Asian coast or than is normal for this time during the winter season.

A partial explanation of this may be found in the two 5-day mean geopotential patterns for 13–17 and 20–24 February 1979 shown in Fig. 5. While the mean longwave pattern along the east coast of Asia is dominated by a broad trough during both pentads, a near reversal is evident in the pattern along the east coast of North America. The intense trough, with an axis near 60° W longitude during the first five-day period, propagates out to sea allowing for rapid building of a ridge along the Atlantic coast of the United States by the second 5-day period. This new pattern then persists for the remainder of the two week study interval. Relaxed baroclinicity and less regionally integrated available potential energy result from the pattern change (Zapotocny, 1985). This pattern change is likely responsible, at least in part, for the lack of significant cyclone formation along the immediate North American coast during this two week period of the FGGE winter season.

Distributions of time-averaged, vertically integrated kinetic energy generation within the North American and Asian regions are shown in Fig. 6. Positive mean $S(K)$ values are generally located along and immediately seaward of the respective coastlines. In a physical sense positive time mean $S(K)$ represents a production of kinetic energy by a thermally direct cell. Thus, the centers of maximum positive mean kinetic energy generation, just off of the eastern coasts of the United States and China, are likely a reflection of the entrance regions to the semi-permanent wintertime jet streaks over the western Atlantic and Pacific oceans, respectively. Likewise, the large areas of negative time mean $S(K)$ located 1500 km or so out to sea from the North American and Asian coasts are probably related to the indirect thermal circulations in the vicinity of the jet exit regions (Murray and Daniels, 1953). For a more complete discussion on the location of these coastal jets during the February 1979 study period, see Zapotocny (1987).

Comparison of the time-averaged $S(K)$ distributions to the composite of cyclone tracks in Fig. 4 indicates fairly good agreement between the areas of positive mean $S(K)$ and the corridors of

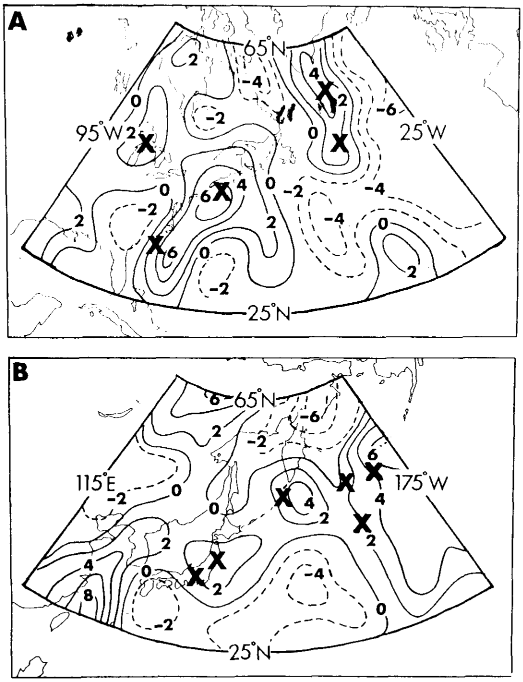

Fig. 6. Same as Fig. 3, but for time-averaged, vertically integrated kinetic energy generation $[S(K)]$ (10 W m^{-2}). X's mark the locations where rapid cyclone deepening (>6 mb/6 h) began.

maximum cyclone activity within each region. Negative mean $S(K)$ values are generally found in the predominant areas of cyclone decay to the south of Iceland in the North American region and east of the Kamchatka Peninsula in the Asian region. Since the regions used in this study are open atmospheric domains, and therefore free to exchange mass and energy with their surroundings, the direct conversion from available potential to kinetic energy cannot be determined from the $S(K)$ alone. Nevertheless, dominance by the transient component of kinetic energy generation can be inferred from the pronounced tendency for $S(K)$ to be a maximum near locations where rapid cyclone deepening commenced (indicated by the X's in Fig. 6). As will be discussed in the following section, intense kinetic energy generation during rapid cyclone deepening events is also evident in the time series of regionally integrated $S(K)$ and of $B(K)$. This, despite the small areal extent of the individual storms as compared to the overall size of the study domains.

Table 1. *Time mean, area-averaged values of regional total available potential energy generation* $[\overline{G(A)}]$

	$\overline{G(A)}$ (W m^{-2})
North American region	5.2
Asian region	−7.4

Time-averaged values of regional total available potential energy (expressed in area-averaged units) in the two study regions are listed in Table 1. The area-averaged mean generation of available potential energy $[\overline{G(A)}]$ is a positive 5.2 W m^{-2} for the North American region, implying relative strong production of baroclinic energy by the diabatic heating distribution in this sector of the northern hemisphere. Somewhat surprisingly, a large negative $\overline{G(A)}$ is indicated for the more cyclogenetically active Asian region, meaning that on average the atmosphere is being heated in regions where the efficiency factor is negative and/or cooled where the efficiency factor is positive. However, since the mean generation of kinetic energy is positive in the Asian region, and because the regional total of available potential energy did not decrease dramatically in the Asian region during the study period (Zapotocny, 1986), it follows that the negative $\overline{G(A)}$ must be offset by the contributions of the pressure work $[W(A+K)]$ and boundary flux $[B(A)]$ terms in eq. 2. The time-averaged sum of $W(A+K)$ and $B(A)$ must be a large positive value in the east Asian sector of the hemisphere during the study period, thereby allowing for the maintenance of the strongly baroclinic environments upon which the developing cyclones depend for their source of kinetic energy.

5. Time series of regionally integrated kinetic energy generation and kinetic energy boundary transport

The vertically integrated $2.5° \times 2.5°$ grid box values of kinetic energy generation were spatially integrated to obtain the twice daily plots of regional $S(K)$ shown in Fig. 7. Considerable variance is evident in both time series. Strong positive generation of regional kinetic energy

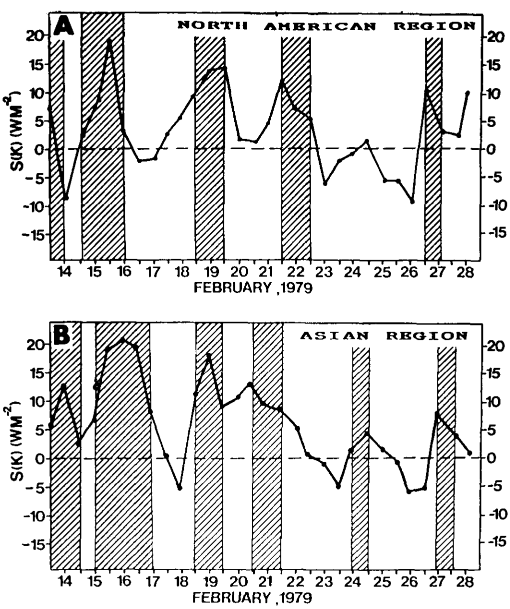

Fig. 7. Time series of area-averaged kinetic energy generation $[S(K)]$ in the North American region (a) and in the Asian region (b) (W m^{-2}). Hatching indicates periods during which rapid cyclone deepening was occurring.

accompanies each of the rapidly deepening cyclones, indicated by the shading in Fig. 7, with small positive or negative generation during the interim periods. Duration of the rapid cyclogenesis episodes ranges from 12 to 48 h. A total of 6 events occurred in the Asian region and 5 in the North American region during the study period. Examination of vertical profiles of $S(K)$ for numerous individual grid boxes (not shown) indicates that lower tropospheric contributions to $S(K)$ are exclusively positive due to the frictionally induced cross-isobar flow always present near the earth's surface. Contributions to $S(K)$ from the middle and upper troposphere change sign as do the regionally integrated values. Positive contributions to $S(K)$ from these levels were generally found to occur several hundred kilometers upstream from the rapidly deepening storm centers, apparently in connection with the thermally direct circulation in the entrance region of the upper-tropospheric jet streak accompanying these cyclones. In the immediate vicinity of the cyclone centers contributions to $S(K)$ above approximately 700 mb were usually negative in response to the indirect ageostrophic

Table 2. *Time mean, area-averaged values of regional kinetic energy generation $[S(K)]$ and kinetic energy boundary transport*

	$\overline{S(K)}$ (W m^{-2})	$\overline{B(K)}$ (W m^{-2})
North American region	3.1	−1.4
Asian region	6.9	2.7

motion induced in the jet streak exit region. Contributions from both the lower and upper troposphere account for the large positive values of regionally integrated $S(K)$ during intense cyclogenesis.

Time-averaged values of regionally integrated kinetic energy generation, as well as kinetic energy boundary transport, are listed in Table 2. Both regions have positive mean generation $[\overline{S(K)}]$. The Asian region value of 8.9 W m^{-2} is nearly 3 times as large as the 3.1 W m^{-2} in the North American region, indicating the more energetically active nature of the Asian coast during the latter half of February 1979. A portion of this difference may again be related to the previously mentioned longwave pattern change and subsequent lack of strong cyclogenesis along the North American east coast during the study period.

The remainder of this section examines the kinetic energy boundary transport term $[B(K)]$ and its relationship to cyclone activity within the study regions. The value of this term is a function of the advection of kinetic energy across the domain boundaries, and is positive (negative) for a net advection of kinetic energy into (out of) a region. Because a net zero transport is assumed at the earth's surface and at the top of the isentropic domains, only the transport through the four vertical walls of each region is considered. Time-averaged values of total kinetic energy transport into the respective regions $[\overline{B(K)}]$ are listed in Table 2. On average for the 15-day study period only the North American region has a negative mean $B(K)$. This indicates that the North American region is exporting more kinetic energy than it imports during the period and acts as a source of kinetic energy for the atmospheric external to the study domain. The Asian region, meanwhile, shows a significant positive value for $B(K)$ and thus represents a sink of hemispheric

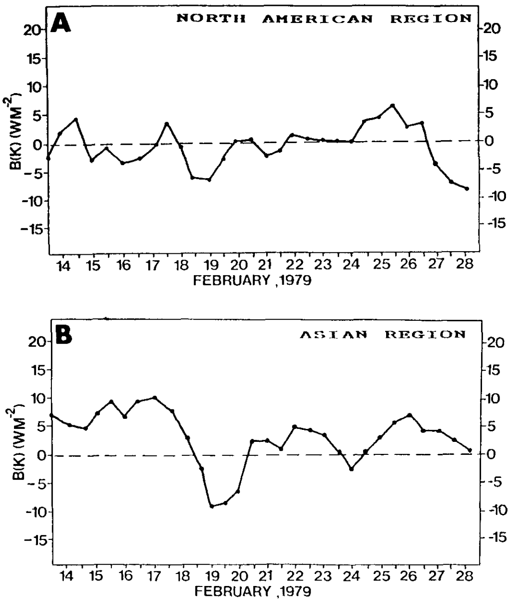

Fig. 8. Time series of area-averaged kinetic energy advection [$B(K)$] into the North American region (a) and Asian region (b) (W m^{-2}).

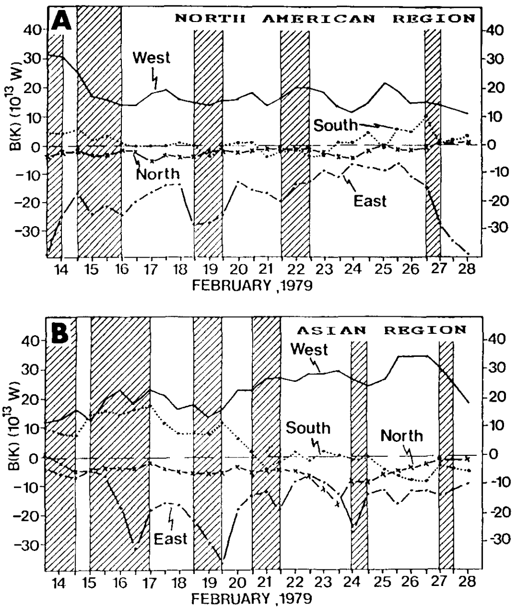

Fig. 9. Same as Fig. 7, except for kinetic energy flux across each of the 4 lateral domain boundaries (10^{13} W).

kinetic energy during the same period of the GWE winter season. From the negative mean boundary transport in the Asian region it can be inferred that frictional dissipation of kinetic energy is stronger on average in that portion of the hemisphere than is the positive generation of kinetic energy, even though the Asian coast is a more active site for strong cyclogenesis with twice as much kinetic energy generated as the North American region.

Time series of total area-averaged $B(K)$ are shown in Fig. 8. The magnitude of this quantity shows considerable daily variance in both study regions. By visual inspection a frequency of approximately 2–3 days is suggested in the Asian region, corresponding quite well to the frequency of intense cyclogenesis (refer back to Fig. 7). However, a clear relationship between the total area-averaged $B(K)$ and individual cyclone occurrences is not discernible in either region. Additional information about the kinetic energy exchange between these regions and their surroundings can be gained by examining the contributions to $B(K)$ by each of the four vertical domain walls. Time series for each of the walls are contained in Fig. 9. For both regions the largest magnitudes of kinetic energy transports, on the order of 30×10^{13} W, are across the western and eastern domain boundaries. Values are exclusively positive for the west face, indicating that only net inward advection of kinetic energy is realized across this boundary. Similarly, the eastern boundary transports are consistently negative, signaling only outward transport through this face. Largest variability in $B(K)$ contributions for both regions occurs for the eastern boundary. Pulsing is evident in the eastern face time series for the Asian region. Here, strong surges of outward kinetic energy transport occur with a frequency of about 2–3 days, and occur nearly simultaneously with episodes of rapid cyclogenesis.

While only the Asian region shows evidence of a possible period to these surges of outward kinetic energy transport, the North American region does have one or two distinct pulses which also appear to be linked to intense cyclogenesis events; most notably, the increase in outward $B(K)$ thru the eastern face of the region during the period of 18–19 February. This corresponds to the time of rapid intensification of the well-studied Presidents' Day storm along the mid-

Atlantic coast of the United States (Bosart, 1981; Uccellini et al., 1984). Inasmuch as the total amount of kinetic energy within the Asian and North American regions showed relatively little change throughout the study period (Zapotocny, 1986), and since the transport into the regions across the other domain walls showed comparatively little variability, it follows, as discussed previously in connection with Fig. 7, that the ultimate source for the large amount of kinetic energy advected out of the regions must be the generation of kinetic energy within the domains during cyclogenesis. This result reiterates the importance of these cyclogenetically active east coast regions in the overall energetics of the northern hemisphere atmosphere.

6. Concluding remarks

This paper has examined some of the interrelationships between extratropical cyclone activity along the eastern coasts of Asia and North America and distributions of available potential energy generation and kinetic energy generation as well as temporal variations in the kinetic energy boundary transport which occurred during a portion of the Global Weather Experiment year. Spatial patterns of time-averaged available potential energy generation showed little correlation to cyclone tracks in either the North American or Asian region. Contrary to the results of some previous studies of available energy generation in these coastal regions, negative time mean $G(A)$ values were noted along the immediate North American east coast during the February 1979 study period, possibly reflecting the relative lack of significant coastal cyclogenesis in that region during this portion of the GWE year. Time-averaged kinetic generation patterns showed a better relationship to cyclone tracks. Maxima in $S(K)$ tended to be co-located with the sites of rapid cyclone deepening, indicating the important contribution by transient features to the time-averaged patterns of $S(K)$. The time-averaged regional totals of available potential energy generation revealed that on average baroclinicity was being enhanced in the North American region but destroyed in the Asian region during the study period by the diabatic heating distributions; however, since the total amount of available potential energy in the regions did not markedly increase or decrease in either region, the time-averaged sum of pressure work and boundary flux must have acted to offset the creation or destruction of available energy thereby maintaining the overall baroclinicity of the regions.

Time series of regionally integrated kinetic energy generation and kinetic energy boundary transport across the vertical walls of the study domains confirmed the significant role these east coast regions play in the energetics of the northern hemisphere. The $S(K)$ time series showed a large increase in regional kinetic energy generation accompanying rapid cyclogenesis events in both regions. Between periods of intense cyclogenesis regional total $S(K)$ occasionally became slightly negative, meaning kinetic energy was being destroyed on average by the ageostrophic component of motion. The $B(K)$ time series indicated surges of outward kinetic energy transport across the eastern face of the Asian region, and to a lesser extent the North American region, which corresponded to the frequency of intense cyclogenesis events with maximum outward transport during or just following the period of most rapid cyclone deepening. The lack of a concurrent or precedent inward flux of kinetic energy, along with the relatively constant values for total regional kinetic energy, verify the fact that the excess kinetic energy was produced within the regions during cyclogenesis. The Asian region, however, was found on average to import more kinetic energy than it exported, and thus represented a sink of hemispheric kinetic energy during this portion of the GWE winter season.

Considerable work remains before a thorough understanding of these relationships or the physical mechanisms responsible for them is realized. This research should include a complete examination of the available potential and kinetic energy budgets within these east coast regions. The limited analysis of budget quantities presented in this paper has raised several interesting points for further investigation, among them the apparent significant role of the pressure work and boundary flux of available potential energy in maintaining a strongly baroclinic environment favorable for cyclogenesis along the Asian east coast. Emphasis in the current study was placed on vertically integrated quantities. A study of energy generations and transports within individual isentropic layers could provide additional insight into the vertical energetics structure of these regions. Finally, several studies including this one have made note of the anomalous atmospheric configuration present over parts of the northern hemisphere, specifically eastern North America, during the GWE winter period. Additional comparisons between energetics in this portion of the northern hemisphere during the GWE winter and other winter seasons are warranted.

7. Acknowledgements

The author wishes to thank Lyle Horn, Donald Johnson and Thomas Koehler for their many helpful comments and suggestions. Special thanks are also extended to Linda Whittaker for supplying the cyclone track data and to Marian Sughrue for typing the manuscript. This research was funded in part through the joint National Science Foundation and National Oceanic and Atmospheric Administration grant ATM-8215035.

REFERENCES

Alpert, J. C. 1981. An analysis of the kinetic energy budget for two extratropical cyclones: The vertically averaged flow and the vertical shear flow. *Mon. Wea. Rev. 109*, 1219–1232.

Bergman, K. H. 1979. Multivariate analysis of temperature and winds using optimum interpolation analysis. *Bull. Am. Meteorol. Soc. 59*, 1603–1611.

Bosart, L. F. 1981. The Presidents' Day snowstorm of 18–19 February 1979: A subsynoptic-scale event. *Mon. Wea. Rev. 109*, 1542–1566.

Bullock, B. R. and Johnson, D. R. 1971a. The generation of available potential energy by latent heat release in a midlatitude cyclone. *Mon. Wea. Rev. 99*, 1–14.

Bullock, B. R. and Johnson, D. R. 1971b. The generation of available potential energy by sensible heating in southern ocean cyclones. *Q. J. R. Meteorol. Soc. 98*, 495–518.

Chen, T. C., Alpert, J. C. and Schlatter, T. W. 1978. The effects of divergent and nondivergent winds on the kinetic energy budget of a midlatitude cyclone: A case study. *Mon. Wea. Rev. 106*, 458–468.

Cressman, G. P. 1984. Energy transformations in the east Asia–west Pacific jet stream. *Mon. Wea. Rev. 112*, 563–574.

Dickson, R. R. 1979. Weather and circulation of February 1979. *Mon. Wea. Rev. 107*, 624–630.

Gall, R. L. and Johnson, D. R. 1971. The generation of available potential energy by sensible heating: A case study. *Tellus 23*, 456–482.

Hahn, D. G. and Horn, L. H. 1969. *The generation of available potential energy in a midlatitude cyclone. Studies of large-scale atmospheric energetics, final report.* ESSA grant WBG-52. University of Wisconsin-Madison, 1–58 pp.

Johnson, D. R. 1970. The available potential energy of storms. *J. Atmos. Sci. 27*, 727–741.

Johnson, D. R. 1989. The forcing and maintenance of global monsoonal circulations: An isentropic analysis. *Advances in Geophysics 31*, in press.

ohnson, D. R. and Downey, W. K. 1982. On the energetics of open systems. *Tellus 34*, 358–470.

Klein, W. H. 1957. Principal tracks and mean frequencies of cyclones and anticyclones in the northern hemisphere. *Res. Paper 40*, U.S. Weather Bureau, U.S. Government Printing Office, Washington, DC, 60 pp.

Koehler, T. L. 1986. A terrain-dependent reference atmosphere determination method for available potential energy calculations. *Tellus 38A*, 42–48.

Koehler, T. L. and Min, K. D. 1984. A study of relationships between available potential energy and extratropical cyclone activity during the FGGE year. *Tellus 36A*, 65–75.

Kung, E. C. and Chan, P. H. 1981. Energetics characteristics of the Asian winter monsoon in the source region. *Mon. Wea. Rev. 109*, 854–870.

Lin, S. C. and Smith, P. J. 1982. The available potential energy budget of a severe-storm producing extratropical cyclone. *Mon. Wea. Rev. 110*, 521–533.

Lorenz, E. N. 1955a. Available potential energy and the maintenance of the general circulation. *Tellus 7*, 157–167.

Lorenz, E. N. 1955b. Generation of available potential energy and intensity of the general circulation. *Large-scale synoptic processes*, Dept. of Meteorology, University of California–Los Angeles.

Margules, M. 1903. On the energy of storms (translated from German by C. Abbe, 1910). *Smithson, Misc. Collect. 51*, 553–595.

McPherson, R. D., Bergman, K. H., Kistler, R. E., Rasch, G. E. and Gordon, D. S. 1979. The NMC operational global data assimilation system. *Mon. Wea. Rev. 107*, 1445–1461.

Min, K. D., Horn, L. H. 1974. The generation of available potential energy by sensible heating along the east coasts of Asia and North America. *J. Meteorol. Soc. Jpn. 52*, 204–217.

Min, K. D., Horn, L. H. 1982. Available potential energy in the northern hemisphere during the FGGE year. *Tellus 34*, 526–539.

Murray, R. and Daniels, S. M. 1953. Transverse flow at entrance and exit to jet streams. *Q. J. R. Meteorol. Soc. 79*, 236–241.

Oort, A. H. 1964. On estimates of the atmospheric energy cycle. *Mon. Wea. Rev. 92*, 483–493.

Oort, A. H. and Peixoto, J. P. 1976. On the variability of the atmospheric energy cycle within a 5-year period. *J. Geophys. Res. 81*, 3643–3659.

Peixoto, J. P. and Oort, A. H. 1974. The annual distribution of energy on a planetary scale. *J. Geophys. Res. 79*, 2149–2159.

Ponater, M. and Speth, P. 1984. Conversions between available potential energy and kinetic energy in January. *Beitr. Phys. Atmosph. 57*, 55–63.

Schaack, T. K. and Johnson, D. R. 1986. Three-dimensional diabatic heating rates during FGGE. In: *National Conf. Scientific Results of the First GARP Global Experiment*. American Meteorol. Soc., 151–154.

Townsend, R. D. and Johnson, D. R. 1985. A diagnostic study of the isentropic zonally averaged mass circulation during the first GARP global experiment. *J. Atmos. Sci. 42*, 1565–1579.

Uccellini, L. W., Kocin, P. J., Petersen, R. A., Wash, C. H. and Brill, K. F. 1984. The Presidents' Day cyclone of 18–19 February 1979: Synoptic overview and analysis of the subtropical jet streak influencing the pre-cyclogenetic period. *Mon. Wea. Rev. 112*, 31–55.

Wei, Ming-Ying, Johnson, D. R. and Townsend, R. D. 1983. Seasonal distributions of diabatic heating during the first GARP Global Experiment. *Tellus 35A*, 241–255.

Whittaker, L. M. and Horn, L. H. 1982. *Atlas of northern hemisphere extratropical cyclone activity, 1958–1977*. Department of Meteorology, University of Wisconsin-Madison, 67 pp.

Whittaker, L. M. and Horn, L. H. 1984. Northern hemisphere extratropical cyclone activity for four mid-season months. *J. Clin. 4*, 297–310.

Zapotocny, J. V. 1985. *Relationships between available potential energy, kinetic energy and extratropical cyclones within limited regions of the northern hemisphere during the FGGE year*. Ph.D. Dissertation, Department of Meteorology, University of Wisconsin-Madison.

Zapotocny, J. V. 1986. Relationships between available potential energy, kinetic energy and extratropical cyclone activity within limited regions of the northern hemisphere during the FGGE year. In: *National Conf. Scientific Results of the First GARP Global Experiment*. American Meteorol. Soc. 101–104.

Zapotocny, J. V. 1987. Relationships between available potential energy, kinetic energy, and extratropical cyclone activity within east coast cyclogenetic regions. *J. Geophys. Res. 97D*, 8401–8410.

Zishka, K. M. and Smith, P. J. 1980. The climatology of cyclones and anticyclones over North America and surrounding ocean environs for January and July 1950–1977. *Mon. Wea. Rev. 108*, 387–401.